Quantum Electronics **41** (1) 86 – 94 (2011)

PACS numbers: 42.55.Px; 42.62.Be; 87.85.–d
DOI: 10.1070/QE2011v041n01ABEH014386

Measurement of micro- and nanovibrations and displacements using semiconductor laser autodynes

D.A. Usanov, A.V. Skripal

Abstract. **The results of theoretical and experimental studies of the possibility to use semiconductor quantum-well lasers, operating in the autodyne regime, for creating nanovibration and nanodisplacement meters are presented. The specific features of the autodyne signal formation under the conditions of strong and weak optical feedback, the influence of current modulation on the shape and spectrum of the autodyne signal, and the methods of measuring the parameters of micro- and nanomotions are described. The description of methods and instrumentation using laser autodynes for the analysis of nanovibration and nanodisplacement parameters of biological objects is presented.**

Keywords: *laser autodyne, interference signal, spectral analysis, wavelet analysis, micro- and nanomotions.*

1. Introduction

Considerable interest to the effect of autodyne detection in semiconductor lasers is caused by the possibility to create simple meters with high sensitivity to the reflected signal on their base [1 – 7]. The system, consisting of a semiconductor laser and an external reflector, combines the functions of an oscillator and an electromagnetic wave detector in one device. The shape of the autodyne signal is, in general, different from that of the interference signal, generated by the same motion of the reflector in an interference system with decoupled radiation source [8 – 13].

Autodyne systems, in general, and semiconductor laser autodynes, in particular, are compact, use no splitting of the light beam into a reference and a measuring one, and do not require alignment of the reference arm and the measuring one because of their coincidence.

Autodyne systems have found application in the displacement control. Their high sensitivity to micro- and nanovibrations and displacements is demonstrated in Refs [14 – 17]. The method of measuring super-small velocities of thermal expansion of solid bodies in a limited time interval on the base of low-frequency spectrum of the autodyne signal is described in [18, 19].

D.A. Usanov, A.V. Skripal N.G. Chernyshevsky Saratov State University, ul. Astrakhanskaya 83, 410012 Saratov, Russia;
e-mail: usanovda@info.sgu.ru, skripalav@info.sgu.ru

Received 25 June 2010; revision received 18 October 2010
Kvantovaya Elektronika **41** (1) 86 – 94 (2011)
Translated by V.L. Derbov

The field of application of autodyne meters becomes substantially wider when the measurements are performed with a high degree of locality. In particular, it becomes possible to determine the parameters of vibration of biological objects, for which the direct measurement of the motion parameters is complicated by the access difficulty [20 – 22]. However, the increase in the reflection locality may raise the level of the external optical feedback, which considerably affects the shape of the autodyne signal of the semiconductor laser oscillator and, therefore, the accuracy of measuring the motion parameters in autodyne systems [23].

One of the advantages of the autodyne system with a semiconductor laser is the possibility to develop systems for measuring the vibrations and displacements using the comparison with an etalon, the role of which is played by the wavelength of the semiconductor laser radiation. In particular, by this method the displacement value or the distance from the reflector can be measured. If the displacement is essentially smaller than the wavelength of the laser radiation, one can apply the method, based on the excitation of additional oscillations with known characteristics [18, 24]. To calibrate the interference signal in an autodyne system one can use modulation of the wavelength of the semiconductor laser radiation, which can be implemented, e.g., by modulating the laser injection current [25].

At present a wider use of autodyne systems for control of vibrations and motions of biological objects is restrained by the difficulties of formation and analysis of the autodyne signal. Examples of biological objects, for which the mentioned techniques was successfully implemented, are the heartbeat of the limnetic crustacean Daphnia, the eyeball tremor, the eardrum vibration. In particular, the semiconductor laser autodyne was used for the diagnostics of pathological conditions of the eardrum. The amplitude-frequency characteristic of the eardrum vibrations at different levels of the sonic action is determined, the difference between the amplitude-frequency characteristics depending on the level of sound pressure in pathological and normal states of the eardrum is ascertained [26 – 28].

The aim of this work is to consider the mathematical methods for analysing the autodyne signal of a semiconductor laser and the possibilities of developing on this base the methods and devices for measuring the characteristics of micro- and nanomotions and displacements.

2. Autodyne signal formation at motion of the external reflector

For a semiconductor laser with external optical feedback (OFB) Lang and Kobayashi [29] proposed a model, in which the laser diode is described by a set of differential equations governing the amplitude and phase of the electromagnetic field and the concentration of charge carriers. For an autodyne system in the cw oscillation regime, when the changes in the system occur during the time much greater than the oscillation period of the electromagnetic radiation, the normalised power of radiation of the semiconductor laser P may be determined using the small-signal analysis of the rate equations (for the complex electric field with retarded argument and the concentration of charge carriers) in the form of a dependence of P on the time $\tau(t)$ of the round trip of the laser radiation over the distance L to the external reflector and back:

$$P = \cos[\omega(t)\tau(t)], \tag{1}$$

where $\omega(t)$ is the frequency of laser radiation. Assuming the roundtrip time of the external resonator to have the form of a harmonic function of time t

$$\tau = \tau_0 + \tau_a \sin(2\pi\nu t + \varepsilon), \tag{2}$$

expression (1) for the variable normalised power of the autodyne signal in the regime of small feedback, when $C \leqslant 1$, can be transformed as

$$P(t) = \cos\{\omega_0\tau_0 + \omega_0\tau_a \sin(\Omega\tau + \varepsilon) - C\sin[\omega\tau_0 + \omega\tau_a \sin(\omega\tau + \varepsilon) + \psi]\}, \tag{3}$$

where C is the level of the external OFB; $\tau_0 = 2L/c$ is the time of laser radiation round trip for the external resonator with an immobile reflector; $\tau_a = 2\xi/c$ is the amplitude of the roundtrip time variation; ξ and $\Omega = 2\pi\nu$ are the amplitude and the frequency of the external reflector vibrations; ε is the initial phase.

Equation (3) describes the normalised power of the autodyne signal, generated in the process of the external reflector vibrations. To describe the spectrum of the autodyne signal in the small feedback regime ($C \leqslant 1$) one can use the Bessel expansion of $P(t)$:

$$P(t) = \cos\theta J_0(\sigma) + 2\cos\theta \sum_{n=1}^{\infty} J_{2n}(\sigma)\cos(2n\Omega t + \varepsilon) - 2\sin\theta \sum_{n=1}^{\infty} J_{2n-1}(\sigma)\cos[(2n-1)\Omega t + \varepsilon], \tag{4}$$

where θ is the phase incursion of the autodyne signal.

The first term in Eqn (4) is a constant component of the autodyne signal. The amplitudes of higher-order harmonics are determined by the quantity σ that enters the expansion and is related to the amplitude of the object vibration by the expression $\sigma = 4\pi\xi/\lambda$, where λ is the wavelength of the laser radiation. To determine the amplitude of the object vibration, the autodyne signal at $C \leqslant 1$ may be also presented in the form of Fourier expansion

$$P(t) = \frac{1}{2}a_0 + \sum_{n=1}^{\infty}[a_{2n}\cos(2n\Omega t) - b_{2n}\sin(2n\Omega t)] - \sum_{n=1}^{\infty}\{a_{2n-1}\cos[(2n-1)\Omega t] - b_{2n-1}\sin[(2n-1)\Omega t]\}. \tag{5}$$

Let us introduce the spectral coefficients S_n in the following way:

$$S_{2n} = 2J_{2n}(\sigma)\cos\theta = \begin{cases} a_{2n}/\cos(2n\varepsilon), & |a_{2n}| > |b_{2n}|, \\ b_{2n}/\sin(2n\varepsilon), & |a_{2n}| < |b_{2n}| \end{cases} \tag{6}$$

for even numbers $2n$ and

$$S_{2n-1} = 2J_{2n-1}(\sigma)\sin\theta = \begin{cases} -a_{2n-1}/\sin[(2n-1)\varepsilon], & |a_{2n-1}| > |b_{2n-1}|, \\ b_{2n-1}/\cos[(2n-1)\varepsilon], & |a_{2n-1}| < |b_{2n-1}| \end{cases} \tag{7}$$

for odd numbers $2n-1$. Here a_n and b_n are the Fourier expansion coefficients; the value of ε is expressed as $\varepsilon = (2n)^{-1}\arctan(b_{2n}/a_{2n})$ for a_n and b_n with even numbers and as $\varepsilon = (2n-1)^{-1}\arctan(-a_{2n-1}/b_{2n-1})$ for a_n and b_n with odd numbers. Note, that the spectral coefficients S_n may be both positive and negative, depending on the values of σ and θ [30].

Using the ratio of expressions (6) and (7), we get the equation determining the amplitude of the reflector vibrations in the form [17]:

$$\frac{S_n}{S_{n+1}} = \frac{J_n(4\pi\xi/\lambda)}{J_{n+1}(4\pi\xi/\lambda)}. \tag{8}$$

The solution of Eqn (8) does not depend on the steady-state phase incursion θ of the autodyne signal, which makes this method convenient for determination of nanometre vibrations of objects. In the case of only three components present in the spectrum of the autodyne signal, expression (8) is reduced to

$$\frac{S_1}{S_3} = \frac{J_1(4\pi\xi/\lambda)}{J_3(4\pi\xi/\lambda)}. \tag{9}$$

As seen from (9), the ratio of the first and the third spectral components depends only on the amplitude of the reflector vibrations. The results of reconstruction of the vibration amplitudes at 5 % random deviation of the interference signal from that calculated theoretically demonstrated that the relative error of the vibration amplitude reconstruction in this case is no greater than 5 %.

Having a high gain and low Q factor, the semiconductor laser autodyne is very sensitive to the changes in the level of the external optical feedback. In [15] the following classification of the regimes of operation of semiconductor lasers with external optical feedback is presented: $C < 0.1$ corresponds to the regime of very weak OFB, the function of the autodyne signal $P(t)$ has the same form as the function of the interference signal in a system with decoupled radiation source (symmetric form); $0.1 < C \leqslant 1$ corresponds to the regime of weak OFB, the function $P(t)$ acquires small distortions and deviates from the symmetric form; $1 < C < 4.6$ corresponds to the regime of moderate OFB, the function $P(t)$ has three values at each moment of time, the autodyne system becomes bistable with two stable states and one unstable state; $C > 4.6$ corresponds to the regime of strong OFB; the function $P(t)$ has five values at each moment of time, and a collapse of coherence may occur in the autodyne system.

Figures 1 and 2 represent the results of calculation of the time dependence of autodyne signals (3) for the levels of optical feedback $C = 0.2, 0.6, 1.0$, as well as the corresponding spectra [23]. The modelling was carried out with harmonic oscillations of the external reflector having the amplitude $\xi = 300$ nm. The analysis of the results shows that, when the level of the external OFB grows, the greater is C the stronger is the distortion of the spectrum of the variable component of the autodyne signal.

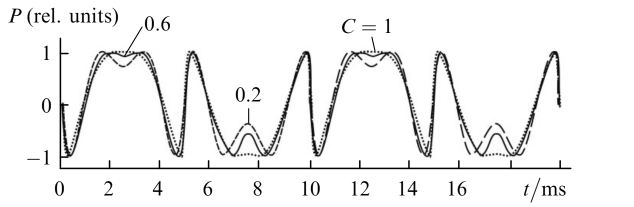

Figure 1. Calculation of the time dependence of autodyne signals (3) for the levels of the external optical feedback $C = 0.2$, 0.6, and 1.0.

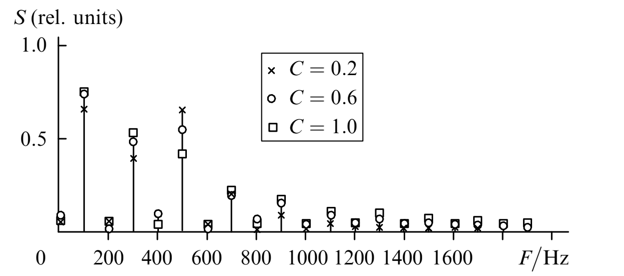

Figure 2. Spectra of the autodyne signals shown in Fig. 1 ($\xi = 300$ nm).

From the analysis of the spectra of the corresponding autodyne signals it follows that the increase in C results in the enrichment of the spectrum and in the change of all harmonics of the autodyne signal, compared to those for $C \ll 1$. Similar enrichment may be observed at increasing the degree of the beam focusing in the plane of the reflector [23], because stronger focusing reduces the fraction of scattered radiation and, correspondingly, increases the power of the returned signal. In [23] it was also shown that a specific feature of the autodyne signal spectrum at $C \ll 1$ is the increase in the number of the spectral component, having the maximal amplitude, with the growth of the object vibration amplitude ξ. At the same time, a slight decrease in the amplitudes of lower-order spectral components is observed. An essentially different character of the spectrum changes is observed when increasing the OFB level. The spectrum enrichment occurs via the increase in the number of spectral components, whose amplitudes are much smaller than those of the dominant one. Under such conditions the number of the harmonic having the maximal amplitude is actually not changed. With the growth of C the shape of the autodyne signal changes in such a way that the spectrum of the autodyne signal acquires the shape, corresponding to a rectangular pulse; the enrichment of the autodyne signal spectrum occurs at the expense of higher-order harmonics (see Fig. 2).

Hence, choosing the distance from the vibrating reflector and adjusting the level of the feedback and the pump current of the laser, one can expand the domain of applicability of the theory of homodyne interferometry, used for determination of the vibration amplitudes by means of autodyne laser systems. As the pump current decreases and approaches the threshold value, it becomes possible to measure the amplitude of the object vibration with enhanced focusing of the beam of the semiconductor laser autodyne. This fact opens the possibility to use the laser autodyne for the determination of the dynamical parameters of biological micro- and nanoobjects.

3. Measurement of the parameters of vibrations with amplitudes comparable with or greater than the laser radiation wavelength

In an interference system the time dependence of the interference signal intensity has the form of a nonharmonic function, even if the object vibrates harmonically, under the condition that the vibration amplitude is comparable with or greater than the laser radiation wavelength. As the object vibration amplitude ξ grows, the enrichment of the spectrum of the detected signal is observed, the amplitude of the dominant harmonic $S_{\max}$ being shifted towards greater harmonic numbers [16]. To derive the amplitude of the object vibrations from the number of the harmonic with the maximal amplitude, it is proposed [16] to use the following approximate expression:

$$\xi = \frac{\lambda}{4\pi}(1.2 + 1.05m), \tag{10}$$

where $m = \omega/\omega_0$ is the number of the harmonic having the maximal amplitude. For the amplitudes not too small ($\xi \geqslant \lambda$) the use of Eqn (10) provides reliable measurements with high accuracy by means of simple measuring systems.

For a semiconductor laser with an external reflector a method is proposed [31] that allows one to reconstruct the interference signal shape, coinciding with that in an interference system with a decoupled radiation source, from the values of the autodyne signal at two phases, corresponding to two distances from the external vibrating reflector. To reconstruct the shape of the mechanical motion of the object from the interference signal in the homodyne interference system with decoupling of the radiation source the known methods for homodyne systems are applied. The technique, described in [31], makes it possible to apply to autodyne systems the methods of determination of the amplitude and the shape of mechanical vibrations of an object, developed for interference system with decoupling of the radiation source, thus widening the region of vibration amplitudes that can be reconstructed from the interferograms in autodyne systems.

In Refs [32, 33] the possibility is demonstrated to solve the problem of reconstruction of a complex nonharmonic periodical motion of the object from the measured time dependences of two interference signals, generated in a laser homodyne system, and the derivative of one of them, using the least square method [34]. The modelling carried out confirmed the possibility to determine the form of the function, describing the motion of the object, by means of the proposed method. The agreement between the calculated and the original shape of the object motion was obtained with the relative error less than 1 %.

The possibility to find the absolute values of the vibration characteristics of mechanical systems, excited by an impact action, without preliminary calibration is studied in Refs [35–37]. The normalised variable component of the interference signal obtained in the autodyne system at $C \ll 1$ can be written as

$$P(t) = \cos\left[\theta + \frac{4\pi}{\lambda} f(t)\right], \tag{11}$$

where λ is the radiation wavelength, $f(t)$ is the object displacement function that can be presented in the form of a Fourier integral:

$$f(t) = \int_{-\infty}^{\infty} c(v)\exp(\mathrm{i}\pi v t)\mathrm{d}v. \tag{12}$$

Here v is the frequency of vibration of the object under study, $c(v)$ is the complex amplitude of the mechanical vibrations at the frequency v. Differentiating $P(t)$ (11), and taking Eqn (12) into account, we get

$$\frac{\mathrm{d}P(t)}{\mathrm{d}t} = -\sin\left[\theta + \frac{4\pi}{\lambda} f(t)\right]\int_{-\infty}^{\infty} \mathrm{i}\,\frac{8\pi^2 v}{\lambda}\, c\exp(\mathrm{i}2\pi v t)\mathrm{d}v. \tag{13}$$

Let us introduce the function $S(t)$, whose spectrum corresponds to that of the reconstructed signal up to a constant factor. Taking Eqn (13) into account, let us present this function in the form

$$S(t) = \frac{\mathrm{d}P(t)/\mathrm{d}t}{\pm\sqrt{1-P^2(t)}} = \int_{-\infty}^{\infty} \mathrm{i}\,\frac{8\pi^2 v}{\lambda}\, c(v)\exp(\mathrm{i}2\pi v t)\mathrm{d}v. \tag{14}$$

From the comparison of the integral forms of the functions $f(t)$ and $S(t)$ we see that the spectral densities of these functions differ by the factor $\mathrm{i}8\pi^2 v/\lambda$. Hence, having constructed the function $S(t)$ on the base of the experimental data, we can find the complex coefficients of the Fourier expansion for the function $f(t)$

$$c(v) = \frac{\lambda}{\mathrm{i}8\pi^2 v}\int_{-\infty}^{\infty} S(\tau)\exp(-\mathrm{i}2\pi v\tau)\mathrm{d}\tau \tag{15}$$

and, using representation (15), reconstruct the function $f(t)$.

The method described above has an essential disadvantage. At the moments of time t_0, when $P(t_0) = 1$, the function $S(t)$, constructed on the base of the interference signal, discontinues. Moreover, in a certain vicinity of these moments of time a distortion of the function $S(t)$ is observed. Using such a function $S(t)$ for determination of the object motion parameters would result in a distortion of the reconstructed law of motion. To apply the method of reconstruction of the object vibration function by means of spectral analysis of the interference signal one should use a continuous function $S(t)$.

To remove the discontinuities and distortions of the function $S(t)$ we suggested that these discontinuities and distortions may be presented as an additive noise in the useful signal. Then the problem of removing the discontinuities of the discussed function is reduced to the problem of its filtering. Two methods of filtering of $S(t)$ were developed, namely, by means of spectral analysis and by means of five-point digital median filtering followed by cubic-spline smoothing

To test the described method of reconstruction of the object motion function we performed the numerical modelling of the reconstruction of a given function, describing the motion of the external reflector. In the course of modelling the function $f(t)$ was given and the interference signal was calculated using Eqn (11). Then the function $S(t)$ was calculated and the inverse problem was solved, namely, the reconstruction of the original function f(t) was carried out, using the technique described above.

The main disadvantage of the method for estimating the parameters of the reflector motion based on the Fourier analysis of the interference signal is that the basis functions, used in the Fourier analysis, are not localised in the time domain. The lack of such a localisation yields errors in the determination of the reflector motion parameters in the case when the reflector vibrations are not periodic. That is why the use of basis functions localised in time and space domains, e.g., wavelets, is of great interest for the analysis of interference signals.

The function representing the longitudinal movements of the object may be written in the integral form

$$f(t) = K_{\Psi_1}^{-1}\int_{-\infty}^{\infty}\int_{-\infty}^{\infty} C_{\mathrm{w}}(a,b)\,\frac{1}{\sqrt{a}}\,\Psi_1\left(\frac{t-b}{a}\right)\frac{\mathrm{d}a\mathrm{d}b}{a^2}, \tag{16}$$

where $C_{\mathrm{w}}(a,b)$ are the coefficients of wavelet expansion of $f(t)$ in the basis Ψ_1 expressed by the formula

$$C_{\mathrm{w}}(a,b) = \int_{-\infty}^{\infty} S(t)\frac{1}{\sqrt{a}}\,\Psi_0\left(\frac{t-b}{a}\right)\mathrm{d}t, \tag{17}$$

and K_{Ψ_1} is the constant, determined by the basis wavelet function

$$K_{\Psi_1} = 2\pi\int_{-\infty}^{\infty}\frac{|\Psi_f(\omega)|^2}{|\omega|}\mathrm{d}\omega. \tag{18}$$

In analogy with the method described above, let us introduce a function $S(t)$ such that its spectrum corresponds to that of the reconstructed signal up to a constant factor

$$S(t) = \frac{\mathrm{d}P/\mathrm{d}t}{\pm\sqrt{1-P^2(t)}}, \tag{19}$$

and express it, taking into account Eqn (11) for the normalised component of the interference signal:

$$S(t) = \frac{4\pi}{\lambda K_{\Psi_1}}\int_{-\infty}^{\infty}\int_{-\infty}^{\infty} C_{\mathrm{w}}(a,b)\,\frac{1}{\sqrt{a}}\,\Psi_2\left(\frac{t-b}{a}\right)\frac{\mathrm{d}a\mathrm{d}b}{a^2}, \tag{20}$$

where Ψ_2 is a derivative of the basis wavelet function Ψ_1.

Below we consider only such wavelet functions $\Psi_1(t)$, whose derivatives are also wavelets. Comparing the integral representations of the functions $f(t)$ and $S(t)$ [Eqns (16) and (20), respectively], one can see that they differ in the basis wavelet function and the constant $4\pi/\lambda$. Having constructed the function $S(t)$ on the base of the interference signal (11), let us expand it over the wavelet basis Ψ_2 to obtain the coefficients $C_{\mathrm{w}}(a,b)$ of the wavelet expansion:

$$C_{\mathrm{w}}(a,b) = \int_{-\infty}^{\infty}\frac{\lambda}{4\pi}\,S(t)\,\frac{1}{\sqrt{a}}\,\Psi_2\left(\frac{t-b}{a}\right)\mathrm{d}t. \tag{21}$$

Then, using the found wavelet coefficients and the basis Ψ_1, let us perform the inverse transformation and get $f(t)$ (16). Hence, using the wavelet transformation of the interference signal, it is possible to estimate the reflector motion parameters in the interference system.

In the course of modelling it was found, that the amplitude of the harmonic motion of the reflector, reconstructed by means of the wavelet method, differs from that of the original motion of the reflector by no more than 5 %, while the frequencies and phases coincide. For comparison, the inverse test problem was solved using the method of reconstruction of the complex motion of the reflector in the interference system by means of the Fourier transform (Fourier method). The deviation of the amplitude of the reflector motion function, reconstructed by means of Fourier method, was no greater than 3 % of the amplitude of the original function, and no difference in frequency and phase was detected.

The case is considered, when the motion of the reflector represents a sequence, each element of which is a harmonic signal, amplitude-modulated by an exponentially damped function. The form of the motion law is illustrated in Fig. 3a. In Fig. 3b a fragment of the registered autodyne signal is presented.

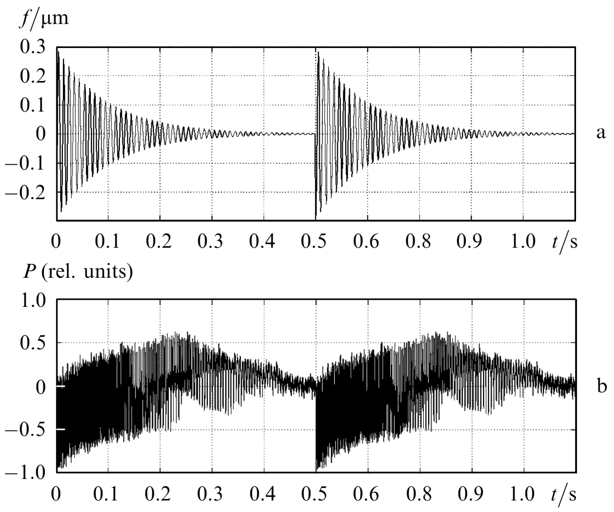

Figure 3. The form of the original object motion function $f(t)$ (a) and the registered autodyne signal $P(t)$ (b).

In the course of modelling the detected signal was processed using the five-point median filtering with subsequent application of the digital Savitsky – Goley filter. The filtered signal is shown in Fig. 4a. The reconstruction of the motion parameters was implemented using the Fourier method. The reconstructed form of the reflector motion law is presented in Fig. 4b. The comparison of the frequencies of exponentially damped oscillations for the original and the reconstructed signal has shown that the frequency difference lies within the measurement error.

4. Autodyne detection of the nanovibration amplitudes

It is convenient to analyse the autodyne signal using spectral methods, in which the amplitude of vibrations is determined from the measured ratio of spectral components or their number [38]. In this case the minimal lower threshold of the measurable vibration amplitudes can be provided using the method, based on the determination of

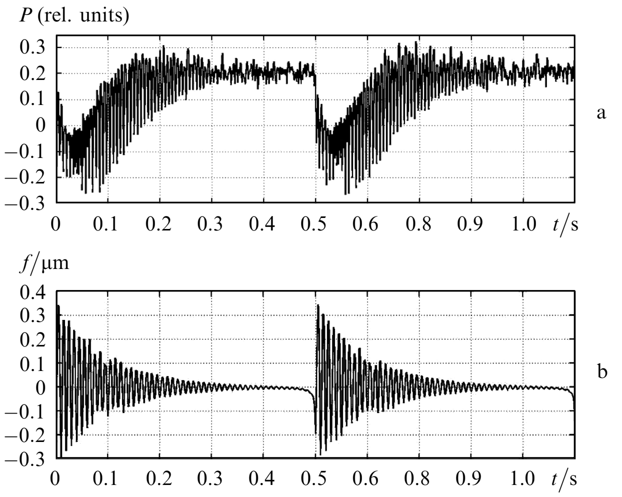

Figure 4. The first two periods of the autodyne signal $P(t)$ after filtering (a) and the first two elements of the sequence of reconstructed function $f(t)$ (b).

the ratio of the first and the third harmonics of the autodyne signal spectrum. Practically, the value of the minimal threshold of such a method is determined by the level of noise, i.e., the value of the object vibration amplitude, at which the third harmonic in the spectrum is detectable against the background of the noise component.

In Ref. [39] it is proposed to determine the object vibration amplitude using the ratio of the first and the second spectral components, which makes is possible to decrease the lower threshold of the measured nanovibration amplitudes. Making use of the autodyne signal normalisation, the equation that determines the object vibration amplitude ξ can be presented in the form

$$\frac{S_1^2}{4J_1^2(4\pi\xi/\lambda)} + \frac{S_2^2}{4J_2^2(4\pi\xi/\lambda)} = 1. \tag{22}$$

Here S_1 and S_2 are the first two harmonics of the spectral expansion of the normalised variable component of the autodyne signal; J_1 and J_2 are the Bessel functions of the first and the second order. Using the components S_1 and S_2, obtained from the expansion of the autodyne signal into a Fourier series, as a result of solution of Eqn (22) we find the amplitude of the object vibration. In this case the experimental measurement of the phase incursion θ of the autodyne signal becomes unnecessary.

An alternative method to determine the characteristics of vibrating objects with nanometre amplitudes is based on the normalisation of the amplitude of the optical radiation, reflected from the vibrating object, or of the amplitude of the spectral expansion harmonic at the frequency of the complementary mechanical vibrations [17]. The registered autodyne signal with the required amplitude is expanded into the first spectral series, and the maximal harmonic in the spectrum is found. Then the amplitude of the object vibrations is gradually increased until the corresponding harmonic reaches the maximum, and then the second spectral series is recorded. To find the desired amplitude of the object vibration, it is possible to use the following ratio of the amplitudes of the spectral components of the autodyne system detector output signal

$$\frac{S_x}{S_n} = \frac{J_n(4\pi\xi_x/\lambda)}{J_n(4\pi\xi/\lambda)}, \tag{23}$$

where S_x is the amplitude of the nth spectral harmonic, whose frequency coincides with that of the studied object vibrations, for the sought amplitude of the reflector vibration ξ_x; S_n is the amplitude of the nth spectral harmonic for the known amplitude of the reflector vibrations ξ. In the case, when the sought vibration amplitude is less than 0.23λ, the relation (23) may be written in the form

$$\frac{S_x}{S_n} = \frac{J_1(4\pi\xi_x/\lambda)}{J_n(4\pi\xi/\lambda)}. \tag{24}$$

The relation (24) is an equation with respect to the unknown variable ξ_x, since S_x and S_n are measured quantities and the vibration amplitude ξ is determined from the normalisation dependence.

In Figs 5 and 6 the measured photo-detected signal and the spectral series for the sought unknown amplitude of the object vibrations are presented. Using the spectrum, presented in Fig. 6, the normalised amplitude of the spectral series at the object vibration frequency ($n = 1$) was found to be $S_x = 0.3931$.

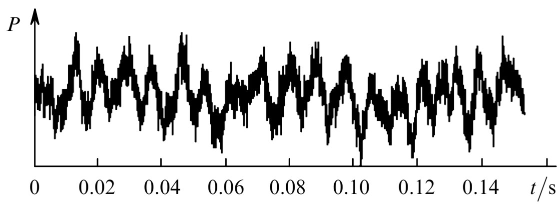

Figure 5. The measured autodyne signal at nanometre amplitudes of the object vibrations.

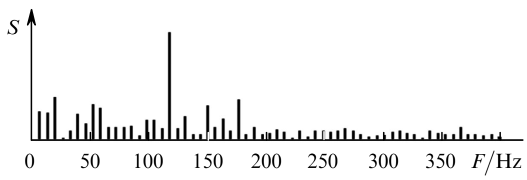

Figure 6. Spectral representation of nanometre amplitudes of the object vibrations.

In Ref. [17] the amplitude of the object vibrations $\xi_x = 1.02$ nm was found from the amplitude of the additional vibration of the object at the maximum of the first harmonic of the autodyne signal spectrum ($\xi = 104$ nm) using Eqn (24). The measurement of smaller amplitudes was limited by the instrumental noises of the measuring setup. It is ascertained, that the proposed autodyne semiconductor laser measuring system allows one to monitor the amplitude of the object vibrations in the range $1 - 10^4$ μm at frequencies from a few Hz to hundreds of MHz. To improve the resolution of the semiconductor laser autodyne system, the selective amplifier U2-8 was used. The measurements have shown that in this case the lower threshold of the measurable amplitudes of the autodyne system is reduced by one more order of magnitude, and the minimal value of measurable amplitude is ~ 1 Å.

The authors of paper [40] showed the possibility to apply the developed method of the autodyne registration of nanometre vibration amplitudes to the quality control of piezoelectric transducers in acoustic delay lines, operating in the microwave frequency region.

5. Measurement of the motion velocity using the autodyne signal spectrum

The velocity of the external reflector motion ϑ can be determined using the spectral component of the autodyne signal at the frequency ν by means of the relation

$$\vartheta = \lambda\nu/2. \tag{25}$$

The applicability of this relation is limited by the fact that the frequency of the variable component of the autodyne signal linearly decreases as the velocity of the object motion becomes smaller.

When measuring super-small velocities of motion, for calibration of the autodyne signal amplitude it is proposed to impart additional vibrations to the object with the amplitude, greater than $\lambda/2$ [41]. In this case the autodyne signal is determined by two components, namely, the slowly varying phase $\theta(t)$ of the autodyne signal and the fast harmonic function $\sigma\sin(\Omega t + \varepsilon)$. If the autodyne signal is analysed using a set of time-limited fragments (time window method), then within each fragment (window) the autodyne signal may be considered to be independent of the slowly varying component $\theta(t)$. Under this assumption the signal analysis is reduced to the determination of the autodyne signal phase for a harmonically vibrating object.

To solve the inverse problem, i.e., to find the phase incursion $\theta(t)$, one can make use of the spectral representation of the autodyne signal in the form of Fourier and Bessel series. To determine the phase incursion of the autodyne signal using four components S_n with subsequent numbers n, one can use the following relations

$$\begin{aligned} \theta_{2n} &= \arctan\left[\frac{(2n+1)}{(2n-1)}\,\frac{(S_{2n+3}+S_{2n+1})S_{2n+1}}{(S_{2n+2}+S_{2n})S_{2n+2}}\right]^{1/2}, \\ \theta_{2n-1} &= \arctan\left[\frac{(2n+1)}{2n}\,\frac{(S_{2n+1}+S_{2n-1})S_{2n+1}}{(S_{2n+2}+S_{2n})S_{2n}}\right]^{1/2}, \end{aligned} \tag{26}$$

where θ_{2n} and θ_{2n-1} are the phases of the autodyne signal, derived from even or odd spectral components of the signal, respectively.

Shifting the chosen time window, within which the analysis of the original signal is performed, along the time axis and calculating the phase incursion of the autodyne signal for each window position, one can get the slowly varying dependence $\Delta\theta(t)$, from which for the known sampling time Δt of the slowly varying component the instantaneous velocity of the moving object is found

$$\vartheta(t) = \frac{\lambda}{4\pi}\,\frac{\Delta\theta}{\Delta t}. \tag{27}$$

In case of an object, moving with a constant velocity, the time dependence of the autodyne signal phase $\Delta\theta(t)$ will be linear.

In Ref. [41] the results of the measurement of linear thermal expansion of a heated sample are presented. To normalise the autodyne signal, the method of imparting harmonic vibrations at the frequency close to 200 Hz by means of a piezoelectric ceramic exciter was applied. The autodyne signal was sampled into window sections with the duration 0.05 s, which were formed by shifting the gate over the autodyne signal with the step 0.01 s. The rate of the object thermal expansion, calculated from the time dependence of the phase incursion change, equals 50 nm s^{-1}.

Hence, the use of quantum-well semiconductor lasers, operating in the autodyne oscillator regime, allows one to monitor the motion of objects with low velocities under the condition of exciting the measured object vibrations with the amplitude, greater than a half of the laser radiation wavelength.

6. Autodyne detection with modulation of the semiconductor laser radiation wavelength

One of the advantages of the semiconductor laser autodyne system is the possibility to create systems for measuring vibrations and displacements by means of the method, in which the measuring signal is compared with the known reference value, e.g., the semiconductor laser radiation wavelength. If the displacement appears to be essentially smaller than the laser radiation wavelength, then the method of superposition of additional oscillation with known characteristics is applied [32]. However, the practical implementation of vibrational motion of the object, the distance from which is to be determined, is not always convenient and possible.

The authors of Ref. [42] proposed to use the periodical modulation of the semiconductor laser radiation wavelength, e.g., by means of modulating the injection current. To determine the phase of the autodyne signal, the expression for the ratio of its even spectral components is used

$$\frac{S_2}{S_4} = \frac{J_1(\sigma) - J_3(\sigma)}{J_3(\sigma) - J_5(\sigma)}, \tag{28}$$

from which the quantity $\sigma = \omega_A \tau$ is found. Then, for known modulation frequency ω_A, the time of passing the distance to the external reflector by the laser radiation, and, hence, the object remoteness $l = c\tau/2$, is calculated (c being the velocity of light).

On the base of this technique, a detailed description of which is presented in Ref. [42], the measurements of the surface profile of an object, placed at a distance of more than 10 cm from the measuring device were carried out with the error of ~ 65 μm. The comparison of the measurement accuracy, provided by the proposed technique, with the performance of known commercial instrumentation demonstrates the benefits of laser autodyne measuring instruments. Thus, the commercial devices do not allow the measurements at distances less than 5 cm, the measurement error in this case approaching 1 mm. As follows from the theoretical analysis, the method and the device, proposed by us, can provide the measurement of distances up to 10 mm with the error not worse than 10 μm. The greater error up to 65 μm, observed in the experiment, is caused by the fact that the accuracy of measuring the distance to the object in the autodyne system depends on the level of OFB. With the increase in the external OFB level the error grows due to the distortion of the shape of the autodyne signal variable component. On the other hand, the decrease in the OFB level in the measuring autodyne system leads to a lower level of the useful signal, compared to the noise. Improving the signal-to noise ratio at lower feedback levels would allow one to increase the accuracy of measuring the distances with an autodyne measuring system.

7. Autodyne interferometry of vibration of biological objects

The results of the study of autodyne detection in semiconductor lasers can be used in monitoring the dynamical states of biological objects. In Refs [43–46] the possibility to apply the interferometry methods to measuring biological vibrations and to problems of cardio diagnostics is discussed. In Refs [45, 46] the mechanism of the output signal formation is studied for the speckle interferometer, aimed at the analysis of vibrations of skin and biological tissues. The results of the theoretical study of the correlation between the structure of phase portraits of the speckle interferometer output signal, caused by the skin surface vibrations, and the severity of cardiovascular diseases are presented in Ref. [46].

In Ref. [22] it is proposed to use a semiconductor laser autodyne for the diagnostics of microsaccadic eye movements (eye tremor), the amplitude of which does not exceed a few microns. The measurements of the interference signal were performed with the semiconductor laser ILPN-206 ($\lambda = 1.3$ μm). The operation regime was chosen such that the radiation power did not exceed 1 mW. The laser radiation, stabilised in power, was incident on the eye sclera surface. The laser was attached to the patient's head with an elastic bandage. The fraction of the radiation, reflected from the surface of the eye sclera, was returned into the laser cavity. The change of the laser output power was measured with a photodetector. The registered autodyne signal is presented in Fig. 7a. As seen from the Figure, the saccade duration was 42 ms, which agrees with the data [22], obtained by photoelectric registration of saccadic movement of the eye.

To register the eye tremor, the measurements were performed in a healthy patient at the moment, when the saccadic movements of the eye were absent. In this case it

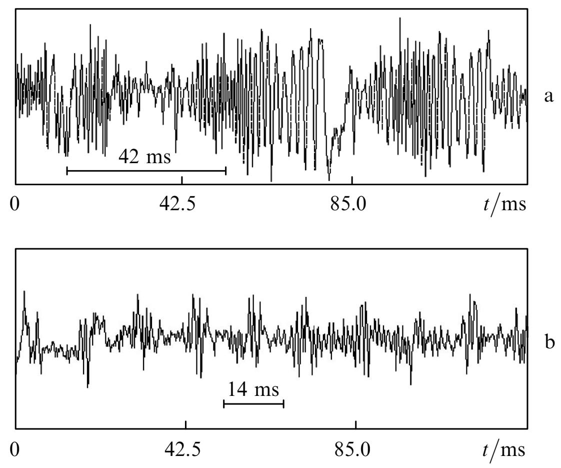

Figure 7. Temporal behaviour of the instantaneous values of normalised detected signal in the cases of saccade (a) and tremor (b).

was possible to detect a periodic motion of the eye with the frequency 72 Hz (the corresponding vibration period being $\sim$ 14 ms). For the registered autodyne interference signal (Fig. 7b) the amplitude of the eyeball vibrations was calculated from the spectrum of the interference signal, presented in Fig. 8. The relation between the object vibration amplitude ξ and the number m of the harmonic, having the maximal amplitude m [Eqn (10)], was used in the calculations. The averaged value of the eye tremor amplitude in a healthy human, calculated in this way, in the direction along the laser beam was 1.4 μm.

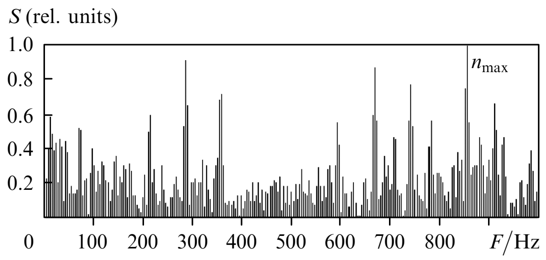

Figure 8. Spectrum of the detected signal of the eye tremor, normalised to the amplitude of the harmonic S_n with the maximal value $m = 12$.

To evaluate the degree of the environmental pollution, the methods based on the evaluation of physiological parameters of test biological objects find wide application. The small limnetic crustacean daphnia (Daphnia magna Straus) is of primary interest as a test object for monitoring the state of aqueous environment, since the high sensitivity of its physiological parameters to the concentration of toxic substances in the aqueous environment is well known [47]. To implement the method, the radiation of a semiconductor laser was focused into the area of the daphnia heart. The measurements of the dependence of the frequency and amplitude of daphnia heartbeats upon the concentration of phenol, diluted in the aqueous environment, revealed substantial advantages of the autodyne registration as a means of test-control of the aqueous medium, aimed at the detection of toxic components, in comparison with the known photoelectric methods.

In Refs [20, 26–28] the possibility is shown to use laser autodyne systems for monitoring the movements of the eardrum. The experimental measurement of the eardrum vibration amplitude was performed using the autodyne measuring system [20], schematically illustrated in Fig. 9. The coherent radiation of the quantum-well RLD-650 laser diode (*5*) ($\lambda = 652$ nm) was incident onto the eardrum (*1*). An expanding funnel was used to provide direct light incidence on the eardrum. The laser radiation, reflected from the eardrum, was detected by the photodetector (*4*), the signal from which passed through the wide-band amplifier (*5*), comprising a filter of variable signal, and was input to the analogue-to-digital convertor (*6*) of the computer (*7*). The sound radiator (*9*), driven by the acoustic vibration generator (*8*), was used to excite the eardrum vibrations.

To study the behaviour of the eardrum at high levels of the acoustic pressure, the spectral composition of the autodyne signal at different intensities of excitation was analysed [28]. Figure 10 shows a fragment of the autodyne signal at the acoustic frequency $\nu_s = 600$ Hz and the level of

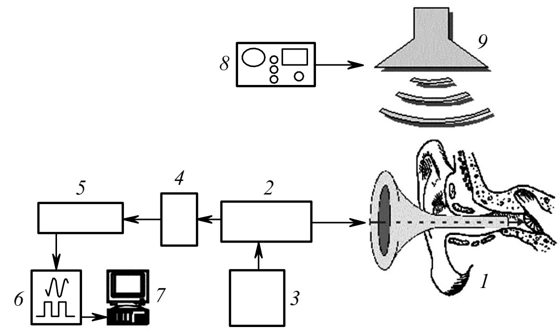

Figure 9. Schematic diagram of the measuring setup: (*1*) eardrum with the funnel expander; (*2*) laser diode; (*3*) pump current source of the laser diode; (*4*) photodetector; (*5*) wide-band amplifier comprising a variable signal filter; (*6*) analogue-to-digital converter; (*7*) computer; (*8*) generator of acoustic vibrations; (*9*) sound radiator.

acoustic pressure 70 dB. In the autodyne signal spectrum (Fig. 11), alongside with the spectral components at frequencies multiple of ν_s, one can observe the spectral components at frequencies multiple of $\nu_s/2$. This allowed us to conclude that at harmonic excitation of the eardrum an additional sub-harmonic appears at half-frequency of the main vibration. The sub-harmonic generation threshold was individual for each patient and was higher than the hearing threshold by 65–75 dB.

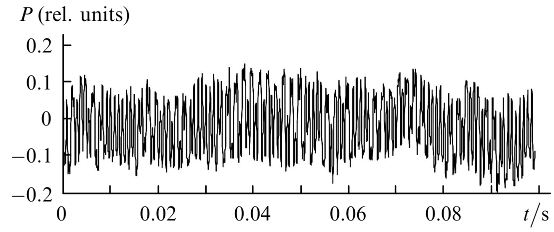

Figure 10. A fragment of the autodyne signal at the frequency of the acoustic action 600 Hz and the level of acoustic pressure 70 dB.

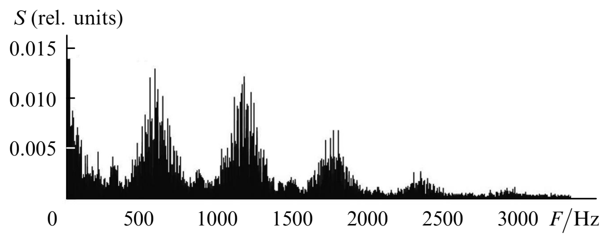

Figure 11. Spectrum of the autodyne signal shown in Fig. 10.

The studies, carried out in a preparation of a pig hearing apparatus, have also shown that with the growth of the excitation amplitude of the eardrum vibrations the sub-harmonic components at frequencies, multiple of the half-frequency of the applied signal, appear in the autodyne signal spectrum. A further increase in the excitation amplitude resulted in the appearance of sub-harmonic components at frequencies, multiple of $\nu_s/4$.

The *in vivo* measurements [48] in humans without hearing pathology (15 persons) and in patients, suffering from bradyacusia (10 persons), have demonstrated that the growth of the vibration amplitude in the ill persons is slower than in healthy humans. The study of the amplitude-frequency characteristic revealed the decrease in the eardrum vibration amplitude in the ill persons, more pronounced in the region of medium and high frequencies.

In Ref. [26] the possibility is shown to diagnose the changes in elasticity and hornification of the tissues of the eardrum in patients with lowered hearing function. The conclusion is made that the presence of visible changes in the amplitude-frequency characteristic of the membrane, registered with the autodyne, opens the possibility to apply the proposed method to the differential diagnostics of bradyacusia.

Paper [27] presents the results of measurements of the longitudinal eardrum displacements, derived from the values of the autodyne signal steady-state phase incursion, found by solving the inverse problem. It was confirmed experimentally that increasing the intensity of the acoustic action on the eardrum causes not only a larger vibration amplitude, but also a longitudinal displacement of the eardrum as a whole.

8. Conclusions

The methods of mathematical description of the autodyne signal of a semiconductor laser are demonstrated and the technologies of monitoring the parameters of micro- and nanomotions are developed on their base. The possibility is demonstrated to apply autodyne systems for the purposes of dynamical state diagnostics of test biological objects, aimed at environmental monitoring, measuring the characteristic frequency and amplitude of the eye tremor, and evaluating the amplitude-frequency characteristics of the eardrum *in vivo*.

References

1. Seko A., Mitsuhashi Y. *Appl. Phys.*, **27**, 140 (1975).
2. Shinohara S., Mochizuki A., Yoshida H., Sumi M. *Appl. Opt.*, **25**, 1417 (1986).
3. Shimizu E.T. *Appl. Opt.*, **26**, 4541 (1987).
4. Jentik H.W., de Mul F.F., Suichies H., Aarnoudse J.G., Greve J. *Appl. Opt.*, **27**, 379 (1988).
5. Mocker H.W., Bjork P.E. *Appl. Opt.*, **28**, 4914 (1989).
6. Semenov A.T. *Kvantovaya Elektron.*, (6), 107 (1971) [*Sov. J. Quantum Electron.*, **1** (6), 652 (1971)].
7. Margin A.V. *Zh. Tekh. Fiz.*, **64**, 184 (1994).
8. Gershenzon E.M., Tumanov B.N., Levit B.I. *Izv. Vyssh. Uchebn. Zaved. Ser. Radiofiz.*, **23**, 535 (1980).
9. Suris R.A., Tager A.A. *Kvantovaya Elektron.*, **11** (1), 35 (1984) [*Sov. J. Quantum Electron.*, **14** (1), 21 (1984)].
10. Tromborg B., Osmundsen J.H., Olesen H. *IEEE J. Quantum Electron.*, **20**, 1023 (1984).
11. Olesen H., Osmundsen J..H., Tromborg B. *IEEE J. Quantum Electron.*, **22**, 762 (1986).
12. Shunc N., Petermann K. *IEEE J. Quantum Electron.*, **24**, 1242 (1988).
13. Bykovskii Yu.A., Dedushenko K.B., Zverkov M.B., Mamayev A.N. *Kvantovaya Elektron.*, **19** (7), 657 (1992) [*Quantum Electron.*, **22** (7), 606 (1992)].
14. Pernick B.J.*Appl. Opt.*, **12**, 607 (1973).
15. Giuliani G., Norgia M., Donati S., Bosch T.J. *Opt. A: Pure Appl. Opt.*, **4**, S283 (2002).
16. Usanov D.A., Skripal A.V., Vagarin V.A. *Prib. Tekh. Eksp.*, **6,** 162 (1994).
17. Usanov D.A., Skripal A.V. *Pis'ma Zh. Tekh. Fiz.*, **9**, 51 (2003).
18. Usanov D.A., Skripal A.V., Kamyshanskii A.S. *Mikroskhem. Tekh.*, **2**, 19 (2004).
19. Usanov D.A., Skripal Al.V., Skripal An.V. *Fizika poluprovodnikovykh radiochastotnykh i opticheskikh avtodinov* (Physics of Semiconductor Radiofrequency and Optical Autodynes) (Saratov: Izdatel'stvo Saratovskogo Universiteta, 2003).
20. Usanov D.A., Mareev O.V., Skripal A.V., Kamyshanskii A.S. *Biomed. Tekh. Radioelektron.*, **8–9**, 94 (2004).
21. Usanov D.A., Skripal Al.V., Vagarin A.Yu., Skripal An.V., Potapov V.V., Shmakova T.T., Mosiyash S.S. *Pis'ma Zh. Tekh. Fiz.*, **24**, 39 (1998).
22. Skripal A.V., Usanov D.A. *Proc. SPIE Int. Soc. Opt. Eng.*, **3908**, 7 (2000).
23. Usanov D.A., Skripal A.V., Avdeev K.S. *Izv. Vyssh. Uchebn. Zaved. Ser. Prikl. Nelin. Dinam.*, **17**, 54 (2009).
24. Usanov D.A., Skripal A.V. Patent of Russian Federation 2208769, priority of 20.07.2003. *Izobreteniya*, No. 20 (2003).
25. Usanov D.A., Skripal A.V., Avdeev K.S. *Pis'ma Zh. Tekh. Fiz.*, **22**, 72 (2007).
26. Usanov D.A., Skripal A.V., Avdeev K.S. *Izv. Vyssh. Uchebn. Zaved. Ser. Prikl. Nelin. Dinam.*, **16**, 41 (2008).
27. Usanov D.A., Skripal A.V., Avdeev K.S., Mareev O.V., Mareev G.O. *Al'manakh Klinicheskoi Meditsiny*, **17**, 358 (2008).
28. Usanov D.A., Mareev O.V., Skripal A.V., Mareev G.O., Kamyshanskii A.S. *Pis'ma Zh. Tekh. Fiz.*, **33**, 90 (2007).
29. Lang R., Kobayashi K. *IEEE J. Quantum Electron.*, **QE-16**, 347 (1980).
30. Vagarin V.A., Skripal A.V., Usanov D.A. *Avtometriya*, (1), 89 (1994).
31. Usanov D.A., Skripal A.V., Kalinkin M.Yu. *Zh. Tekh. Fiz.*, **70**, 125 (2000).
32. Gangnus S.V., Usanov D.A., Skripal A.V. *Proc. SPIE Int. Soc. Opt. Eng.*, **3726**, 226 (1998).
33. Usanov D.A., Skripal A.V., Gangnus S.V. *Avtometriya*, (1), 117 (2001).
34. Gangnus S.V., Usanov D.A., Skripal A.V. *Proc. SPIE Int. Soc. Opt. Eng.*, **4002**, 151 (2000).
35. Skripal A.V., Chanilov O.I., Usanov D.A. *Izv. Vyssh. Uchebn. Zaved. Ser. Prikl. Nelin. Dinam.*, **1**, 79 (2005).
36. Chanilov O.I., Usanov D.A., Skripal A.V. *Pis'ma Zh. Tekh. Fiz.*, **31**, 9 (2005).
37. Skripal A.V., Chanilov O.I., Usanov D.A. *Avtometriya*, (5), 56 (2004).
38. Pernick B.J. *Appl. Opt.*, **12**, 607 (1973).
39. Usanov D.A., Skripal A.V., Kamyshanskii A.S. *Pis'ma Zh. Tekh. Fiz.*, **32**, 42 (2006).
40. Usanov D.A., Skripal An.V., Sergeev A.A., Abramov A.N., Skripal Al.V., Abramov A.F., in *Mater. Nauchno-Tekhnich. Konf. 'Perspektivnyye Napravleniya Razvitiya Elektronnogo Priborostroyenuya'* (Saratov, 2003) p. 153.
41. Usanov D.A., Skripal A.V., Kamyshanskii A.S. *Mikroskhem. Tekh.*, **2**, 19 (2004).
42. Usanov D.A., Skripal A.V., Avdeev K.S. *Pis'ma Zh. Tekh. Fiz.*, **3**, 72 (2007).
43. Fercher A.F., Hu H.Z., Steeger P.F. Briers J.D. *Opt. Acta*, **29**, 1401 (1982).
44. Ryabukho V.P., Tuchin V.V., Ul'yanov S.S., Zimnyakov D.A. *Proc. SPIE Int. Soc. Opt. Eng.*, **2100**, 19 (1994).
45. Ul'yanov S.S., Ryabukho V.P., Tuchin V.V. *Opt. Eng.*, **33**, 908 (1994).
46. Ul'yanov S.S., Tuchin V.V. *Izv. Vyssh. Uchebn. Zaved. Ser. Prikl. Nelin. Dinam.*, **2**, 44 (1994).
47. Kiknadze G.S., Yesakov B.P., Ruz'minykh S.B., Komarov V.M. *Opyt otsenki stepeni zagryazneniya vodnoy sredy po izmeneniyam perioda biyeniya serdtsa dafnii* (Experience of Evaluation of Aqueous Medium Pollution via the Change of Heartbeat Period in Daphnia) (Pushchino: Izd. Nauchnogo Tsentra Biol. Issl. Akademii Nauk SSSR, 1983) p. 13.
48. Mareev O.V., Mareev G.O., Usanov D.A., Skripal A.V. *Meditsinskii Al'manakh*, **3**, 49 (2008).